Pharmacodynamic Analysis of Target Inhibition and Endothelial Cell Death in Tumors Treated with the Vascular Endothelial Growth Factor Receptor Antagonists SU5416 or SU6668

Darren W. Davis,[1] Ryan Takamori,[1] Chandrajit P. Raut,[1] Henry Q. Xiong,[2] Roy S. Herbst,[3] Walter M. Stadler,[7] John V. Heymach,[6] George D. Demetri,[6] Asif Rashid,[4] Yu Shen,[5] Sijin Wen,[5] James L. Abbruzzese,[2] and David J. McConkey[1]

Departments of [1]Cancer Biology, [2]Gastrointestinal Medical Oncology, [3]Thoracic Head & Neck Medical Oncology, [4]Pathology, and [5]Biostatistics, University of Texas M.D. Anderson Cancer Center, Houston, Texas; [6]Department of Medical Oncology, Dana-Farber Cancer Institute and Harvard Cancer Center, Boston, Massachusetts; and [7]Department of Medicine, University of Chicago, Chicago, Illinois

ABSTRACT

Purpose: **To determine the effects of small molecule inhibitors of vascular endothelial growth factor receptor (VEGFR)-2 (SU5416 and SU6668) on receptor phosphorylation in tumor xenografts and in paired tumor biopsies obtained in three clinical trials in patients with advanced solid malignancies.**

Experimental Design: **The dose-dependent effects of SU6668 on angiogenesis and tumor growth were investigated in orthotopic L3.6pl pancreatic tumors. Excisional or 18G core biopsies were obtained from patients before and after therapy with SU5416 or SU6668. Laser scanning cytometry–mediated analysis was used to quantify levels of phosphorylated and total VEGFRs and platelet-derived growth factor receptors (PDGFR), tumor microvessel densities, vessel sizes, and endothelial and tumor cell apoptosis.**

Results: **Significant inhibition of tumor microvessel density and growth and increased apoptosis were observed at SU6668 maximum tolerated dose (100 mg/kg) in L3.6pl xenografts. At 6 hours post therapy, SU6668 reduced VEGFR and PDGFR phosphorylation in the tumors by 50% and 92%, respectively, but levels rebounded beyond the baselines by 24 hours. Levels of phosphorylated VEGFR-2 and PDGFR also decreased significantly (≈50%) 6 hours after therapy in 1 of 6 primary human tumors treated with SU6668, but these effects were not associated with increased apoptosis. A significant increase in endothelial cell apoptosis was observed in one tumor exposed to SU5416 and was associated with an increase in vessel size, but these changes occurred without an increase in tumor cell death.**

Conclusions: **SU5416 and SU6668 displayed biological activity in xenografts. However, neither drug produced marked biological activity in primary patient tumors.**

INTRODUCTION

Angiogenesis is critical for the growth of solid tumors (1–5). Tumor angiogenesis is dependent on the production of proangiogenic cytokines that are produced by the tumor cells themselves and by stromal cells (4, 5). Most prominent among these bioactive polypeptides is vascular endothelial growth factor (VEGF; ref. 6), which plays essential roles in the proliferation, migration, differentiation, and survival of endothelial cells. The effects of VEGF on endothelial cells and subsequent tumor vascularization seem to be mediated via its engagement of VEGF receptor (VEGFR)-2, also known as KDR or Flk-1 (6). Thus, compounds that target the ligand-receptor (VEGF-VEGFR-2) interaction and VEGFR-2-mediated signal transduction are being developed aggressively for cancer therapy.

SU5416 was the first small molecule inhibitor of VEGFR-2 to be evaluated in large-scale clinical trials (7, 8). The compound is a competitive inhibitor of the ATP-binding site in the VEGFR-2 tyrosine kinase domain (K_i=0.16 μmol/L; ref. 9). It displays 20-fold selectivity for VEGFR-2 compared with the structurally related platelet-derived growth factor receptor (PDGFR), and it displays almost no activity against the receptors for epidermal growth factor or basic fibroblast growth factor (9). SU6668 is a second-generation synthetic derivative of SU5416 (10) that displays somewhat less activity against VEGFR-2 (K_i=2.1 μmol/L) but also inhibits the receptors for basic fibroblast growth factor (K_i=1.2 μmol/L) and PDGF(K_i=8 nmol/L; ref. 11). Both compounds were tested in xenograft models in which they attenuated tumor growth via inhibition of angiogenesis (10, 12–15). Pharmacodynamic analysis of their effects in these models linked tumor growth inhibition to VEGFR-2 and PDGFR blockade and induction of apoptosis in tumor-associated endothelial cells (14, 15).

The overall purpose of the present study was to characterize the effects of SU5416 and SU6668 on relevant pharmacodynamic markers associated with inhibition of receptor activation and angiogenesis. Both drugs were evaluated previously in

Received 4/22/04; revised 10/4/04; accepted 10/27/04.
Grant support: NIH/National Cancer Institute grants U54 CA090810 (D.J. McConkey), U01 CA62461 (J.L. Abbruzzese), and CA16672 and CA91846 (Y. Shen), the Golfers Against Cancer (R.S. Herbst), the Commonwealth Foundation for Cancer Research (D.W. Davis), Sugen, Inc., and National Cancer Institute, Department of Health and Human Services, research grant CA16672 [to the confocal microscopy and image analysis core facility (M. Andreeff, M.D., Ph.D., Director) and core laboratory (C. D. Bucana, Ph.D., Director)].
The costs of publication of this article were defrayed in part by the payment of page charges. This article must therefore be hereby marked *advertisement* in accordance with 18 U.S.C. Section 1734 solely to indicate this fact.
Requests for reprints: David J. McConkey, Department of Cancer Biology, Unit 173, University of Texas M.D. Anderson Cancer Center, 1515 Holcombe Boulevard, Houston, TX 77030. Phone: 713-792-8591; Fax: 713-792-8747; E-mail: dmcconke@mdanderson.org.

clinical trials, and the antitumor activity observed did not meet expectations (16–19). However, because pharmacodynamic analyses of target inhibition were not done, it was not clear whether the lack of significant clinical activity was due to a poor choice of drug targets or to ineffective target inhibition.

Previous studies showed that human L3.6pl pancreatic tumor xenografts express VEGF and PDGF and inhibitors of VEGFR-2 and PDGFR attenuate their growth via inhibition of angiogenesis (20–22). Here we used laser scanning cytometry (LSC; refs. 23–25) to determine the extent of VEGFR-2 and PDGFR blockade associated with SU6668-mediated inhibition of growth and angiogenesis in orthotopic L3.6pl tumors. We then used the same methods to measure the effects of SU5416 and SU6668 on VEGFR-2 and PDGFR phosphorylation and downstream markers of angiogenesis inhibition in matched pre- and posttreatment biopsies obtained in three clinical trials. Together, the results indicate that the biological activity observed in response to patient therapy with either drug was lower than that associated with growth inhibition in the L3.6pl tumors. These observations probably explain the lack of clinical activity observed in the single-agent trials done with these drugs in patients.

PATIENTS AND METHODS

Effects of SU6668 on Orthotopic L3.6pl Xenografts. The L3.6pl human pancreatic cancer cell line was derived from COLO-357 (26). The cells were used to generate orthotopic tumors as described previously (26, 27). Tumors were implanted in 6-week-old male, athymic nude mice (25-30 g) that were obtained from the Animal Production Area of the National Cancer Institute, Frederick Cancer Research Facility (Frederick, MD). Mice were housed in groups of five in laminar flow cabinets under specific pathogen-free conditions in facilities approved by the American Association for Accreditation of Laboratory Animal Care and in accordance with current regulations and standards of the U.S. Department of Agriculture, U.S. Department of Health and Human Services, and NIH, and their use in these experiments was approved by the Institutional Animal Care and Use Committee. One week after tumor implantation, mice were randomized into four treatment groups (10 mice per group). The mice were given daily i.p. injections of sterile normal saline or one of three SU6668 doses (25, 50, or 100 mg/kg), all in 100-μL volumes. The mice were euthanized after 21 days of treatment (postoperative day 28). Body and tumor weights were measured. Part of the tissue was fixed in formalin and embedded in paraffin; the rest was embedded in optimal cutting temperature (OCT) compound (Miles, Elkhart, IN), frozen rapidly in liquid nitrogen, and stored at −70°C.

Tumor microvessel densities (MVD) were quantified by anti-CD31 immunohistochemistry as described previously (27). Briefly, paraffin sections (4-6 μm thick) were mounted on positively charged Superfrost slides (Fisher Scientific, Co., Houston, TX) and dried overnight. Sections were deparaffinized in xylene, followed by treatment with a graded series of alcohol [100%, 95%, 80% ethanol/double-distilled water (v/v)] and rehydrated in PBS (pH 7.5), treated with pepsin (Biomeda, Foster City, CA) for 15 minutes at 37°C, and washed with PBS. Immunohistochemical procedures were done as described previously (28). Positive reactions were visualized by incubating the slides with stable 3,3′-diaminobenzidine for 10 to 20 minutes. The sections were rinsed with distilled water, counterstained with Gill's hematoxylin (colorimetric development) and mounted with Universal Mount (Research Genetics, Birmingham, AL). Tumor microvessels were counted in five randomly selected high-power fields located in the tumor periphery in sections obtained from each of the tumors in each treatment group.

To determine the effects of SU6668 on VEGFR-2 and PDGFR phosphorylation, established (7-day) orthotopic L3.6pl tumors were treated daily with 100 mg/kg SU6668 or vehicle control for 3 weeks. Tumors were harvested from mice (n = 5 per group) at 6 and 24 hours after the last dose of SU6668, embedded in OCT compound, frozen rapidly in liquid nitrogen, and stored at −70°C.

Immunofluorescence Measurements of Phosphorylated and Total VEGFR-2, PDGFR-β, or EGFR. Active VEGFR-2 was quantified using a phosphorylation site–specific antibody corresponding to amino acid residues 1170 to 1180 of the human VEGF receptor (Ab-1, Oncogene, La Jolla, CA) as described previously (25). Active PDGFR-β was measured in the same manner using a goat anti-phosphorylated PDGFR-β antibody (Tyr^{1021}, Santa Cruz Biotechnology, Santa Cruz, CA). Control experiments were done with a goat anti-phosphorylated EGFR antibody (Tyr^{1173}, Santa Cruz). Total receptor levels were measured using a rabbit anti-VEGFR-2 (C1158, Santa Cruz), a rabbit anti-PDGFR-β (P20, Santa Cruz), or a rabbit anti-EGFR (1005, Santa Cruz) antibody. Prolong (Molecular Probes, Eugene, OR) was used to mount coverslips.

Immunofluorescence CD31 (Endothelial Cells) and Terminal Deoxynucleotidyl Transferase–Mediated Nick End Labeling. Apoptosis in tumor and endothelial cells was quantified by three-color immunofluorescence staining and LSC analysis as described previously (24, 25). Tissues were first stained with a monoclonal anti-human CD31 (clone JC/70A, Dako Corporation, Carpinteria, CA) and a Cy5-conjugated goat anti-mouse secondary (Jackson ImmunoResearch Laboratories, West Grove, PA). Fluorescent terminal deoxynucleotidyl transferase–mediated nick end labeling (TUNEL, Promega, Madison, WI) was done as described previously (24, 25). Finally, cell nuclei were counterstained with 1 μg/mL propidium iodide for 5 minutes. Tissues were then washed with PBS twice for 3 minutes and Prolong (Molecular Probes) was used to mount coverslips.

Laser Scanning Cytometry Analysis. The laser scanning cytometer (CompuCyte Corporation, Cambridge, MA) is an instrument designed to enable fluorescence-based quantitative measurements on tissues at the single-cell level (23–25). The instrument consists of a base unit containing an Olympus BX50 fluorescent microscope and an optics unit coupled to an argon and HeNe laser. Thus, the laser scanning cytometer was used very much like a fluorescence-activated cell sorter to obtain three-color immunofluorescence intensity information from the heterogeneous tissue specimens. Before LSC analysis, all biopsies were pathologically confirmed for the presence of tumor cells by H&E staining, tumor regions were selected for data acquisition, and all tissues were evaluated for the quality of immunofluorescence staining. Each slide was placed on the computer-controlled motorized stage and the desired tumor area to be scanned was

visually located using the epifluorescence microscope of the instrument, excluding normal and necrotic tissue regions.

For quantitative analysis of apoptosis, levels of phosphorylated or total VEGFR-2, PDGFR, or EGFR, the threshold contour was set to optimize single cell contours. Slides were scanned using a ×200 objective and cell nuclei were contoured using the red fluorescence (propidium iodide) detector. The long red fluorescence detector was used to detect Cy5 fluorescence and the green detector was used to detect FITC fluorescence. The relative levels of fluorescence for each antigen were plotted on a scattergram. Analytic gates were used to define four quadrants that determine the total number of cells within each population (e.g., $CD31^-/TUNEL^+$ versus $CD31^+/TUNEL^+$, or total $VEGFR\text{-}2^+/p\text{-}VEGFR\text{-}2^+$ versus total $VEGFR\text{-}2^+/p\text{-}VEGFR\text{-}2^-$, etc.). Each gate was set based on the fluorescent properties of the negative control sample (IgG or secondary immunofluorescent antibody). The relocation feature was used to confirm that the cells positive for each antigen were included in the appropriate gates. The data files were replayed to determine the percentage of each cell population (e.g., apoptotic tumor-associated endothelial cells or tumor cells) in each biopsy. Results for VEGFR-2, PDGFR, or EGFR are represented as the ratio of the phosphorylated form to the total form of the protein for normalization of change in total receptor levels.

Tumor MVD and vessel size were quantified by LSC as described previously (25). Immunofluorescence detection of microvessels was achieved by staining with anti-CD31 according to the previous CD31/TUNEL protocol. The desired area to be scanned was visually located using the epifluorescence microscope of the instrument, excluding normal and necrotic tissue regions. Slides were scanned using a ×200 objective and microvessels were contoured using the long red fluorescence detector. The threshold contour was set to optimize single-vessel contours based on contiguous immunofluorescence of the secondary antigen. A negative control sample was used to establish a gate for negative and positive vessels. The total number of microvessels was determined for each biopsy, and MVD was calculated by the ratio of microvessels normalized to the total number of tumor cells in the same region (obtained from a subsequent scan counting total cell nuclei). To measure the size of each vessel within the tumor tissue section, the data file was replayed with the area/perimeter ratio selected on the *X* axis of the histogram window.

SU5416 Trials. A detailed description of the Dana-Farber clinical trial design is provided elsewhere (18). Patients 7 to 9 were all diagnosed with measurable metastastic or inoperable soft tissue sarcomas. Patients treated with SU5416 at the University of Chicago (patients 10 and 11) had refractory, progressive metastatic melanoma and were required to have normal organ function (17). Patients with serious coronary artery disease, recent myocardial infarction, severe peripheral vascular disease, or history of arterial or venous thrombosis in the last 3 months were excluded. Patients could have no medical contraindications to high-dose steroids, and all provided written, signed, informed consent. The clinical protocol was approved by the Cancer Therapy Evaluation Program under a contract from the National Cancer Institute to the University of Chicago, and was approved by the University of Chicago Cancer Research Center Clinical Trials Review Board and the relevant institutional review boards as well.

Patients in both trials were treated with SU5416 145 mg/m^2 i.v. over 30 minutes twice weekly for 8 weeks. To prevent cremaphor hypersensitivity patients also received dexamethasone (10 mg p.o.) before and 12 hours after each SU5416 infusion. Patients were monitored with liver function tests and electrolytes every other week, and with physical examination, complete blood count, and corticotropin stimulating test every 4 weeks. Radiologic scans for disease evaluation were done at baseline and every 8 weeks, and standard Response Evaluation Criteria in Solid Tumors defined response and progression.

SU6668 Trial. Patients with solid malignancies who failed or no longer responded to available conventional treatment were eligible for this study (19). Patients were required to have accessible tumor lesions that were amenable to core needle biopsy. Six patients per dose level were planned for treatment with SU6668 at 200, 400, and 600 $mg/m^2/d$ in divided doses daily without interruption. The accrual was stopped before the goal was reached due to toxicity that was observed at higher dose levels at other institutions and subsequent termination of the further clinical development of SU6668. Patients continued on treatment until unacceptable adverse events, symptomatic disease progression, or disease progression more than 100% (by unidimensional measurement) in the absence of symptoms. All patients underwent routine laboratory evaluation (including complete blood count and evaluation of liver and renal function), routine radiographic imaging, functional computed tomography, dynamic contrast-enhanced magnetic resonance imaging, and core needle biopsy of tumors. During treatment, patients had routine laboratory test, history, and physical examination every 4 weeks (one cycle). The clinical protocol was approved by the Cancer Therapy Evaluation Program under a contract from National Cancer Institute to the University of Texas M.D. Anderson Cancer Center and was approved by the institutional review board. All patients enrolled in the study provided a written, signed, informed consent.

Tumor Biopsies. All patients consenting to the SU6668 treatment protocol were required to participate in a protocol assessing various end points of angiogenesis inhibition, including tumor biopsy analysis (19). Tumor biopsies were optional for patients enrolled in either of the SU5416 treatment protocols and were limited to patients with masses at least 2 cm in diameter (17, 18). Regardless of the treatment protocol, only those patients considered to have a low risk for complications by the performing physician underwent a biopsy procedure. A detailed description of patient characteristics, disease type, and the biopsy characteristics, including organ site and timing, is provided in Table 1. Biopsies were obtained from 11 tumors, 6 from patients treated with SU6668 (daily, 200 mg/m^2) at M.D. Anderson Cancer Center (patients 1-6) and 5 from patients treated with SU5416 (twice weekly, 145 mg/m^2, patients 7-11). All of the SU6668 tissues were snap frozen in OCT, whereas all of the SU5416 biopsies were formalin fixed and paraffin embedded. Posttreatment biopsies were obtained within 6 hours after the last dose of SU6668 from all of the patients treated with this drug, whereas the timing of posttreatment biopsy acquisition was variable in the SU5416 studies, ranging from 3 to 9 days after dosing (Table 1).

Table 1 Patient, tumor, and biopsy characteristics

Patient	Age	Sex	Diagnosis	Agent/Dose (mg/m2)	Site of biopsy	Baseline biopsy, size/no. of cells analyzed	Posttreatment biopsy, days after initiation of treatment/ days after last dose/size/no. of cells analyzed
1	65	F	Metastatic colorectal cancer to the liver	SU6668, 200 daily	Liver	18G (1 pass)/441	Day 39/< 6 h after last dose/18G (1 pass)/1,608
2	58	M	Metastatic melanoma	SU6668, 200 daily	Peritoneal	18G (1 pass)/199	Day 29/<6 h after last dose/18G (1 pass)/215
3	52	F	Metastatic colorectal cancer to the liver	SU6668, 200 daily	Liver	18G (1 pass)/1,516	Day 33/<6 h after last dose/18G/ (2 pass)/931
4	84	M	Metastatic colorectal cancer to the liver	SU6668, 200 daily	Liver	18G (2 pass)/242	Day 28/<6 h after last dose/18G (1 pass)/1,512
5	28	F	Malignant melanoma, unknown primary	SU6668, 200 daily	Chest wall	18G (2 pass)/378	Day 31/<6 h after last dose/18G (2 pass)/217
6	66	F	Metastatic leiomyosarcoma to abdomen/liver	SU6668, 200 daily	Abdominal wall	18G (2 pass)/2,520	Day 28/<6 h after last dose/18G (2 pass)/3,257
7	55	M	GIST	SU5416, 145 2x wk	Liver	0.2 to 1.3 cm cores (5 pass)/25,820	Day 63/3 days after last dose/0.3 × 0.7 cm cores (2 pass)/24,444
8	72	F	Angiosarcoma, right chest wall	SU5416, 145 twice a week	Right chest wall	1 × 0.4 × 0.6 cm/58,411	Day 45/9 days after last dose/1.2 × 0.8 × 0.8 cm/84,960
9	49	F	Leiomyosarcoma	SU5416, 145 twice a week	Uterus	1.9, 1.8 cm cores (2 pass)/9,343	Day 60/4 days after last dose/2.1, 1.4 cm cores (5 pass)/24,009
10	49	M	Melanoma	SU5416,145 twice a week	Lymph node	1 × 2 cm/25,481	Day 65/2 days after last dose/3 × 3 cm/46,212
11	59	F	Melanoma	SU5416, 145 twice a week	Soft tissue/arm	2 × 2 cm/21,028	Day 56/3 days after last dose/3 × 4 cm/25,535

NOTE. Patients enrolled on the M.D. Anderson Cancer Center SU6668 trial (patients 1-6) were required to provide 18G core biopsies at study entry and after one cycle of therapy. Patients 7 to 9 were enrolled on the SU5416 trial at the Dana-Farber Cancer Institute (soft tissue sarcomas), and patients 10 to 11 received SU5416 at the University of Chicago (melanomas). Note that the posttreatment biopsies in the SU5416 trial were obtained at days 45 to 63 and 2 to 9 days after the last dose of drug. Abbreviation: GIST, gastrointestinal stromal tumor.

Statistical Analyses. For the xenograft studies, statistical analysis was done using the InStat Statistical Software version 3.05 (San Diego, CA). A P value < 0.05 was considered statistically significant. In the biopsy, analyses baseline and posttreatment values were determined by averaging the percentage of each cellular population obtained in three sequential biopsy sections from the SU6668 trial and three regions of interest in two separate biopsy sections from the SU5416 trials. An independent sample t test was used to determine the variability of pharmacodynamic biomarkers in each biopsy. A linear regression model was used to fit the relationship between the baseline and posttreatment values for each biomarker. The Wilcoxon signed rank exact test was used to evaluate whether treatment-induced changes in any biomarker was significant in tumors exposed to SU6668 ($n = 6$), SU5416 ($n = 5$), or both treatment types ($n = 11$). Differences between values were considered significant for $P < 0.05$. Due to the small sample sizes for the study, the statistical analyses are descriptive in nature.

RESULTS

Effects of SU6668 on Orthotopic L3.6pl Pancreatic Tumors. Previous studies have shown that therapy with an inhibitor of VEGFR-2 and PDGFR (PTK-787) inhibits the growth of orthotopic L3.6pl pancreatic tumors via induction of endothelial cell death and inhibition of angiogenesis (20, 21). We therefore studied the effects of SU6668 on the tumor growth and receptor phosphorylation in orthotopic L3.6pl tumors to determine the level of receptor inhibition associated with therapeutic activity. Established (7-day) tumors (10 mice per group) were treated daily with increasing doses of SU6668 (25-100 mg/kg), and tumor volumes were measured after 21 days of therapy. Therapy resulted in no gross signs of toxicity, and body weights among the four treatment groups were very similar (data not shown). Consistent with results obtained in other xenograft models (10, 14), the highest dose of SU6668 (100 mg/kg) produced significant inhibition of tumor growth (40% decrease), whereas lower doses were ineffective (Fig. 1*A*). Growth inhibition in response to

100 mg/kg SU6668 was associated with a significant reduction in tumor MVD (26% decrease; Fig. 1*B*) and increased levels of endothelial cell (Fig. 1*C*) and tumor cell death (Fig. 1*D*; 5- and 1.7-fold, respectively).

In a second experiment we tested the effects of 100 mg/kg SU6668 on VEGFR-2 and PDGFR phosphorylation in L3.6pl xenografts. Preliminary studies were done with human umbilical vein endothelial cells to optimize immunofluorescent detection of phosphorylated VEGFR-2 using a phosphorylation site–specific antibody (data not shown). Two-color immunofluorescent staining showed that active VEGFR-2 was confined to CD31+ (endothelial) cells (data not shown), whereas active PDGR was present in CD31+ and CD31− cells (Fig. 2*A*). Quantitative LSC analyses showed that baseline levels of PDGFR-2 phosphorylation were higher in the endothelial cells compared with the levels observed in tumor cells (Fig. 2*B*). SU6668 produced a 50% inhibition of VEGFR-2 and PDGFR phosphorylation in endothelial cells 6 hours after therapy (Fig. 2*B* and *C*). The effects of SU6668 on PDGFR phosphorylation at 6 hours were more dramatic in tumor cells (92% inhibition, Fig. 2*B*). These results are consistent with the relative IC_{50} values of the drug against VEGFR-2 (2 μmol/L) versus PDGFR (8 nmol/L) and the observation that baseline PDGFR phosphorylation levels were lower in the tumor cells as compared with the endothelial cells (Fig. 2*B*). Strikingly, although 100 mg/kg SU6668 produced the expected inhibition of VEGFR and PDGFR phosphorylation at 6 hours, levels of receptor phosphorylation were significantly higher than controls in the SU6668-treated tumors 24 hours after drug dosing (Fig. 2*A*-*C*). These results show that SU6668-mediated inhibition of receptor phosphorylation was not sustained *in vivo* and that levels actually "rebounded" beyond the baseline prior to each administration of the drug.

Effects of SU5416 and SU6668 on Receptor Phosphorylation in Primary Tumors. We next measured receptor phosphorylation and biomarkers of angiogenesis inhibition in biopsies collected within the context of clinical trials of SU6668 (patients 1-6) or SU5416 (patients 7-11; Table 1; Fig. 3). To ensure that only those sections of the core biopsies that contained viable tumor cells were selected for data acquisition, all samples were stained with H&E and reviewed by a pathologist. In some cases, none of the biopsy tissue was evaluable, and these cores were excluded from the analyses. Larger biopsies were available from the SU5416 studies because they involved patients with more accessible solid tumors (soft tissue sarcomas, melanoma; Table 1). Tissue sections stained with the anti-phosphorylated VEGFR-2 and total VEGFR-2 antibodies were also visually inspected to verify the quality of immunofluorescent antigen

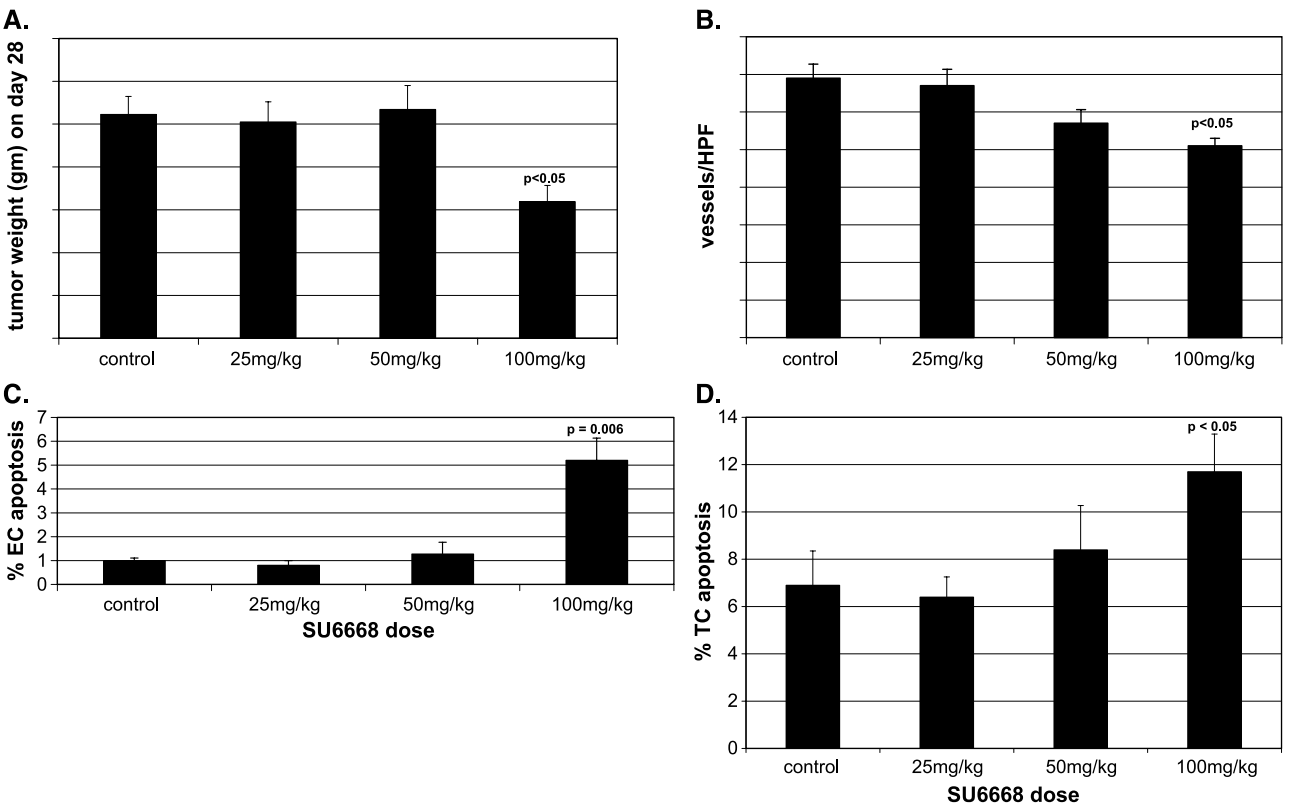

Fig. 1 Effects of SU6668 on orthotopic L3.6pl tumors. *A,* dose-dependent effects on tumor weights. Animals bearing established (7-day) orthotopic L3.6pl tumors were treated daily with 25, 50, or 100 mg/kg SU6668 via i.p. injection for 21 days. Animals were then sacrificed and tumors were harvested and weighed. Columns, mean (n = 10); *bars,* SE. *, $P < 0.05$. *B,* effects of SU6668 on tumor MVDs. Tumor sections were stained with an anti-CD31 antibody and tumor MVDs were quantified in the tumor peripheries by immunohistochemistry. Five high-power fields (*HPF*) were analyzed in each tumor. Columns, mean (n = 10); bars, SE. *C,* effects of SU6668 on endothelial cell apoptosis. Tumor sections were double-stained with anti-CD31 plus TUNEL, and percentages of CD31+TUNEL+ cells were quantified by LSC. Columns, mean (n = 10); bars, SE. *D,* effects of SU6668 on tumor cell death. Percentages of CD31-TUNEL+ cells were measured by LSC. Columns, mean (n = 10); bars, SE.

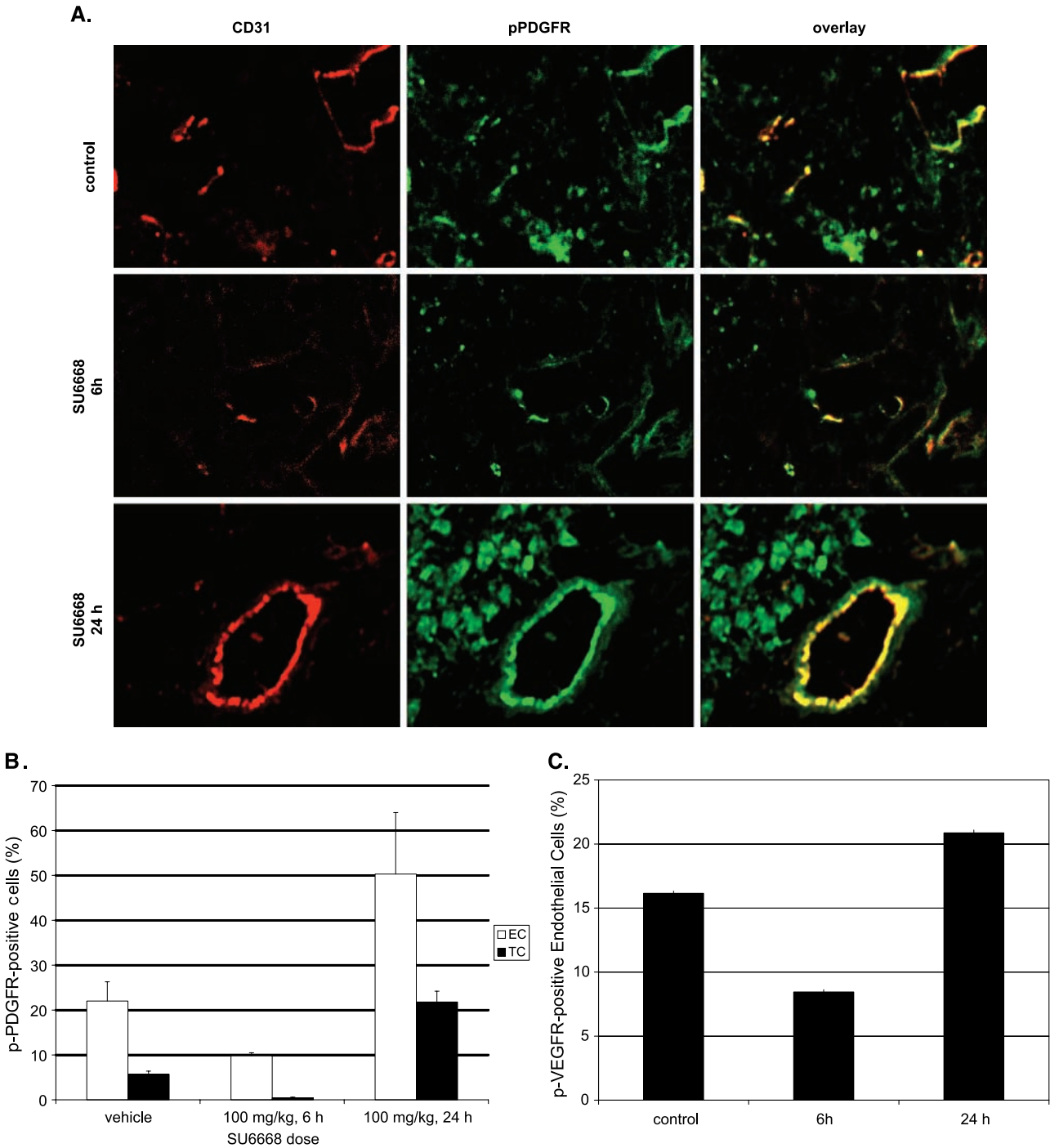

Fig. 2 Quantification of phosphorylated VEGFR-2 and PDGFR levels in L3.6pl xenografts by LSC. *A,* representative immunofluorescent images of phosphorylated PDGFR in L3.6pl tumors treated with SU6668. Tumor sections were stained with anti-CD31 (*red, left*) and anti-phosphorylated PDGFR-β (*green, middle*) as described in PATIENTS AND METHODS. Overlays (*right*) display colocalized CD31 and phospho-PDGFR-β in endothelial cells, which appear yellow. Note reduction in phosphorylated PDGFR-β in tumor and endothelial cells at 6 hours and the increased levels observed at 24 hours after SU6668 therapy. *B,* effects of SU6668 on PDGFR phosphorylation. Tissues were stained with anti-CD31 and anti-phosphorylated PDGFR-β as described in PATIENTS AND METHODS, and levels of fluorescence in CD31+ and CD31− cells were quantified by LSC; □, endothelial cells; ■, tumor cells. Columns, mean (n = 3); bars, SD. *C,* LSC-mediated quantitative analysis of the effects of SU6668 on phosphorylated VEGFR-2. Levels of phosphorylated VEGFR-2 were measured as described in PATIENTS AND METHODS. Columns, mean (n = 5); *bars,* SD.

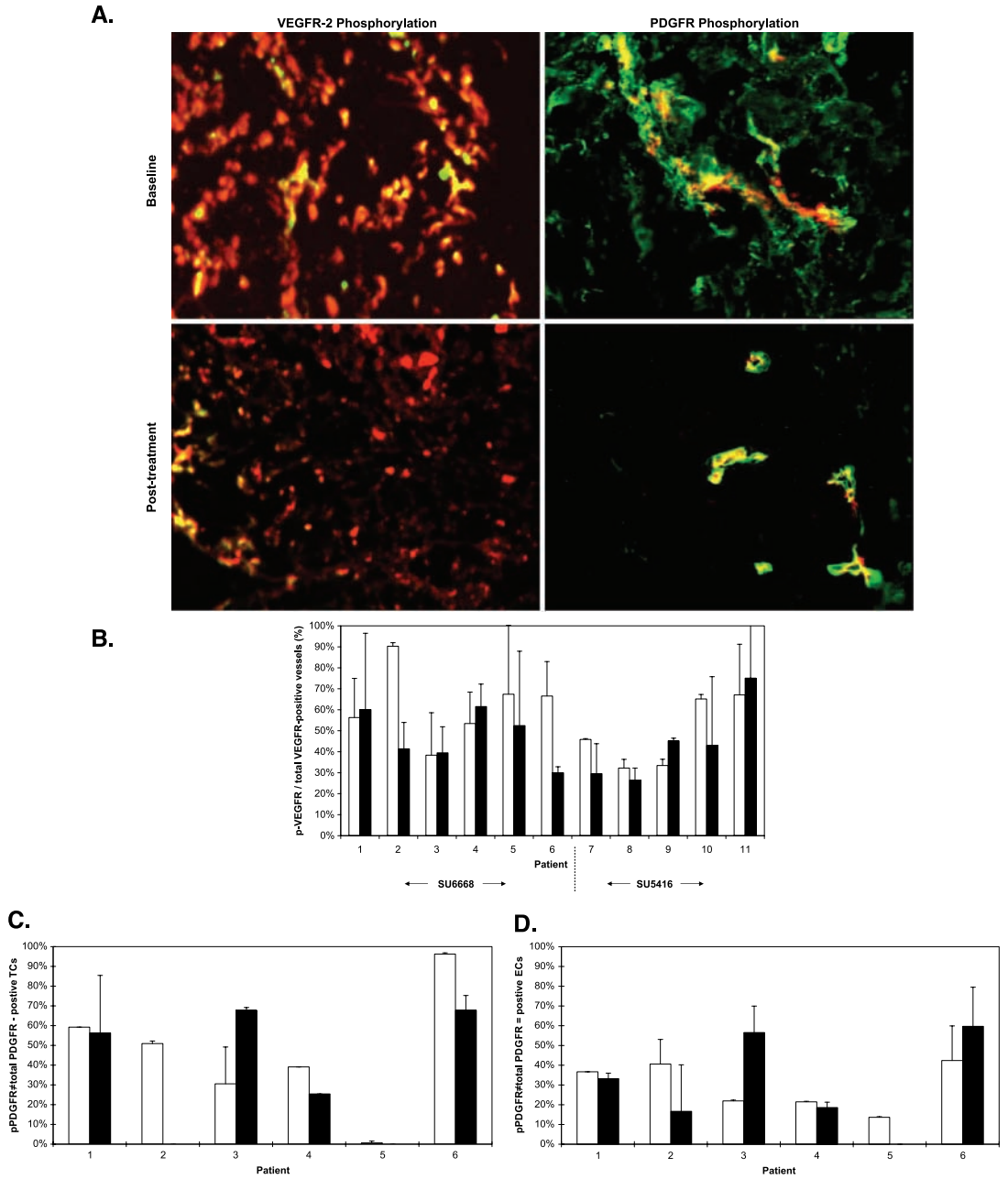

Fig. 3 Quantification of VEGFR-2 and PDGFR phosphorylation in primary patient tumors by LSC. *A,* immunofluorescent detection of phosphorylated VEGFR-2 or PDGFR. Tissue sections were stained with antibodies specific for phosphorylated and total VEGFR-2 or PDGFR as described in PATIENTS AND METHODS. *Left,* representative LSC-generated images showing phosphorylated VEGFR-2 levels (*green*) superimposed on total VEGF receptor (*red*) levels before and after SU6668 therapy. Colocalization of phosphorylated VEGFR-2 and total VEGFR appears *yellow*. In this particular tumor (patient 2), SU6668 treatment reduced VEGFR-2 phosphorylation. *Right,* representative LSC-generated images of phosphorylated PDGFR (*green*) levels superimposed on tumor-associated endothelial cells (CD31/*red*) before and after SU6668 therapy. Colocalization of phosphorylated PDGFR and CD31 appears *yellow*. In this tumor from patient 2, SU6668 treatment reduced PDGFR phosphorylation, especially in the tumor cells (CD31-negative). *B,* quantitative analysis of VEGFR-2 activity. Phosphorylated and total VEGFR-2 levels were quantified by LSC-mediated analysis as described in PATIENTS AND METHODS. Data acquisition included three to five regions in two to three sequential biopsy sections from each tumor that contained viable tumor cells. Data are represented as a percentage of total tumor microvessels positive for phosphorylated VEGFR-2 to total VEGFR-2. □, mean of pretreatment levels; ■, mean of posttreatment levels. *Bars,* SD. *C,* phosphorylated and total PDGFR levels in tumor cells (CD31-negative) were quantified by LSC-mediated analysis as described in PATIENTS AND METHODS. Data acquisition included three to five regions in two to three sequential biopsy sections from each tumor that contained viable tumor cells. The data represent the percentages of total tumor cells that were positive for phosphorylated PDGFR relative to total PDGFR levels. □, mean of pretreatment levels; ■, mean of posttreatment levels. *Bars,* SD. *D,* phosphorylated and total PDGFR levels in tumor endothelial cells were quantified by LSC-mediated analysis as described in PATIENTS AND METHODS. Data acquisition included three to five regions in two to three sequential biopsy sections from each tumor that contained viable tumor cells. Data are represented as a percentage of total tumor endothelial cells positive for phosphorylated PDGFR relative to total PDGFR. □, mean of pretreatment levels; ■, mean of posttreatment levels. *Bars,* SD.

detection by LSC (Fig. 3*A*). These sections were then subjected to quantitative analysis by LSC (Fig. 3*B*). At baseline, phosphorylated VEGFR-2 was detected in 30% to 90% of CD31-positive tumor-associated microvessels. Exposure to SU6668 was associated with significant (≥50%, $P < 0.001$) reductions in phosphorylated VEGFR-2 in two of the six tumors (Fig. 3*B*, patients 2 and 6), whereas levels were not significantly different ($P > 0.05$) in the other four. In contrast, we did not detect significant changes in levels of VEGFR-2 phosphorylation in any of the five paired biopsy sets obtained from patients treated with SU5416 (Fig. 3*B*). There was no statistically significant effect on VEGFR-2 phosphorylation levels when the average pre- and posttreatment levels were compared for either the SU6668- ($n = 6$, $P = 0.4375$) or the SU5416- ($n = 5$, $P = 0.625$) treated patients, or when levels were averaged across the entire panel ($n = 11$, $P = 0.2061$).

We then analyzed levels of PDGFR phosphorylation in the paired biopsies obtained from the six patients treated with SU6668 (Fig. 3*A*). Levels were highly variable at baseline (3-95% positive cells; Fig. 3*C* and *D*). Interestingly, levels of PDGFR phosphorylation were lower in the tumor (Fig. 3*C*) and endothelial (Fig. 3*D*) cell compartments in one of the biopsy sets (patient 2) that displayed a significant reduction in phosphorylated VEGFR-2 (Fig. 3*B*). Other pairs of biopsies displayed posttreatment decreases in PDGFR phosphorylation in either the tumor cell (patients 4 and 6) or endothelial cell (patient 5) compartment. However, in the case of tumor 6 the level of phosphorylated PDGFR increased slightly in the endothelial cell compartment, and the reductions in PDGFR phosphorylation observed in tumors 4 and 5 were not associated with parallel decreases in phosphorylated VEGFR-2 (Fig. 3*B*). Therefore, we conclude that SU6668 produced measurable receptor inhibition (VEGFR-2 plus PDGFR) in only one of six primary tumors (tumor 2). There was no statistically significant overall effect on PDFGR phosphorylation levels when the average pre- and posttreatment levels for all tumors were compared for either tumor cells ($P = 0.3125$) or endothelial cells ($P = 1$). Levels of phosphorylated EGFR were indistinguishable in all of the pre- and posttreatment tissues (data not shown).

Effects of SU5416 and SU6668 on Tumor Microvessels. We quantified tumor MVDs in our panel of paired biopsy sets by immunofluorescent anti-CD31 staining and LSC analysis (Fig. 4*A*; refs. 24, 25). They were variable at baseline, ranging from less than 10% to almost 80% (Fig. 4*B*). The MVDs were somewhat lower in 5 of the 11 posttreatment biopsies relative to matched baseline biopsies. Interestingly, the greatest decrease in MVD was observed in the tumor (tumor 2) that displayed parallel reductions in phosphorylated VEGFR-2 and PDGFR in response to SU6668 therapy (Fig. 4*B*). However, there was no statistically significant overall effect on MVDs when the average pre- and posttreatment levels were compared for either SU6668- ($n = 6$, $P = 0.3125$) or SU5416- ($n = 5$, $P = 0.125$) treated patients or across the entire panel ($n = 11$, $P = 0.1475$).

Effects of SU5416 and SU6668 on Microvessel Size. In a recent study, we found that the blocking anti-VEGFR-2 antibody DC101 caused an increase in mean vessel size associated with growth inhibition in orthotopic human 253J B-V bladder tumor xenografts (25). These observations are consistent with others suggesting that angiogenesis inhibitors preferentially affect smaller, less well differentiated blood vessels in tumors (29). To compare relative vessel volumes in the tumor sections, we used the LSC contour feature to determine mean vessel sizes (area/perimeter ratios) in the baseline and posttreatment tissue sections. The results revealed no change in mean vessel sizes in 10 of the 11 biopsy sets, including tumor 2 (Fig. 4*C*, *left*). Mean vessel size did increase in one of the tumors (tumor 9), identified as a rightward shift in the vessel size histogram (Fig. 4*C*, *right, red trace*). This tumor was also among the five that displayed a significant reduction in MVD (Fig. 4*B*).

Effects of SU5416 and SU6668 on Apoptosis. Effective therapy with SU5416 or SU6668 in tumor xenografts was associated with significant increases in apoptosis in both tumor and endothelial cells (Fig. 1*C* and *D*; refs. 14, 15). Therefore, in a final series of analyses, we quantified levels of endothelial cell and tumor cell apoptosis in the biopsies obtained in the SU5416 and SU6668 clinical trials. Biopsies were stained with an anti-CD31 antibody and TUNEL and counterstained with propidium iodide to detect all cell nuclei. Each biopsy was visually inspected to ensure that nonspecific background staining was minimal and that the quality of staining was optimal for laser scanning analysis (Fig. 5*A*). Quantitative analysis of all biopsies revealed that baseline levels of endothelial cell death were uniformly low (<3%, Fig. 5*B*), consistent with our previous observations in another clinical trial (24). Comparison of pre- and posttreatment biopsies revealed significant increases in endothelial cell apoptosis in only 1 of 11 tumors (tumor 9, Fig. 5*B*). This tumor was the same one that showed an increase in mean vessel size (Fig. 4*C*). Quantification of apoptosis levels in the CD31-negative cells revealed no increases in any of the tumors (Fig. 5*C*). Specifically, in no case did treatment-induced tumor cell death approach 10%, a level that correlated with tumor regression in a previous study done with tissues obtained as part of a clinical trial of neoadjuvant therapy in patients with breast cancer (23). Importantly, levels of endothelial and tumor cell apoptosis were lower after SU6668 therapy in the biopsy set obtained from tumor 2 (Fig. 5*B* and *C*), the only one that displayed parallel decreases in activated VEGFR-2 and PDGFR levels (Fig. 2).

DISCUSSION

VEGFR-2 plays an obligate role in tumor angiogenesis, placing it among the most attractive therapeutic targets in cancer (30, 31). Because they displayed promising activity in preclinical models, SU5416 and SU6668 were selected to be the first small molecule inhibitors of VEGFR-2 to be evaluated in National Cancer Institute–sponsored clinical trials. Although there was some evidence for antitumoral activity in some patients treated with SU5416 (32, 33), dose-escalation trials with SU6668 were halted because of drug toxicity in the absence of obvious clinical activity. However, the extent of receptor inhibition was not determined in any of the trials. Thus, it has been impossible to determine whether the lack of clinical activity observed with both agents was due to a poor choice of targets (VEGFR-2), ineffective target inhibition, or an uncoupling of target inhibition from downstream biological responses (i.e., cell death).

We initiated the present study to address these questions. We developed highly sensitive, automated methods for the

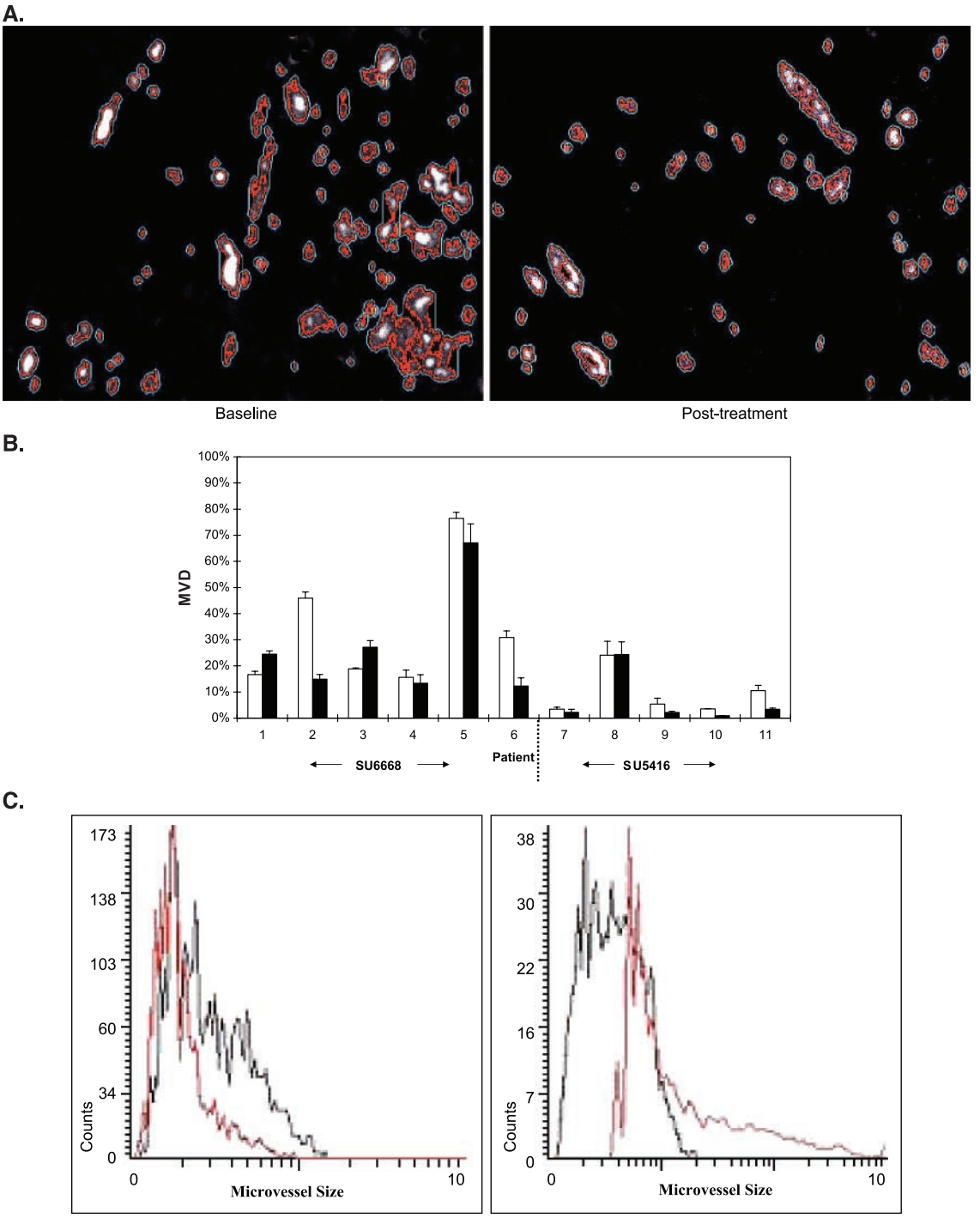

Fig. 4 Effects of SU5416 and SU6668 on tumor microvessels in primary tumors. *A,* identification of microvessels by LSC-mediated contouring of contiguous anti-CD31 immunofluorescence as described in PATIENTS AND METHODS. Biopsy regions containing viable tumor cells were scanned by LSC to quantify tumor microvessels. Representative LSC-generated images show detection of microvessels (*white*) with single vessel contours (*red outline*). In this tumor pair from patient 2, SU6668 reduced tumor MVD. *B,* quantification of tumor MVD. Microvessel densities were determined in three to five regions in two to three sequential biopsy sections from each tumor that contained viable tumor cells. □, pretreatment levels; ■, posttreatment levels. Posttreatment MVDs were significantly lower compared with pretreatment levels in tumors from patients 2, 6, 9, 10, and 11. *Columns,* mean; *bars,* SD. *C,* determination of mean vessel sizes. LSC-mediated contouring analysis of microvessels in *A* was used to measure each tumor vessel size (area/perimeter ratios) in each biopsy section. Representative histograms show mean vessel size before treatment (*black outline*) and after therapy with SU5416 or SU6668 (*red outline*). *Left,* results obtained from patient 2 (representative of 10 of 11 tumors analyzed); *right,* results from tumor 9. Note the shift in mean vessel size following treatment with SU5416.

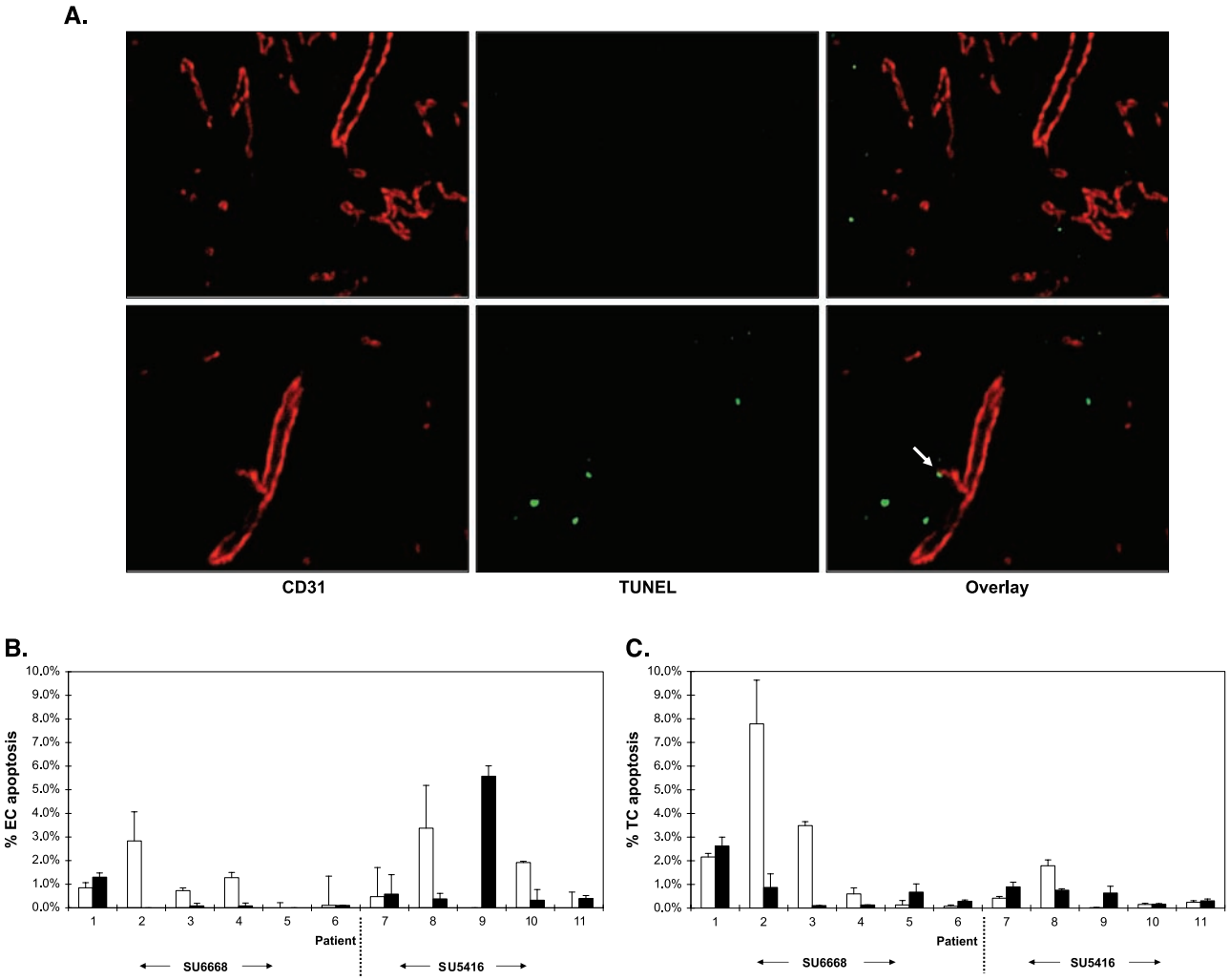

Fig. 5 Effects of SU5416 and SU6668 on apoptosis in primary tumors. *A,* detection of apoptotic cells by fluorescent TUNEL analysis. Biopsies were stained with an anti-CD31 antibody (*red*) and TUNEL (*green*) as described in PATIENTS AND METHODS. The representative LSC-generated scanned image reveals characteristically low levels of apoptosis in endothelial cells (*arrow*) and tumor cells (CD31-negative) before (*top*) and after (*bottom*) SU5416 therapy. Results are representative of the quality of staining obtained with all of the tissue sections. *B,* LSC-mediated quantification of endothelial cell apoptosis. Percentages of $CD31^+/TUNEL^+$ cells (relative to the total number of $CD31^+$ cells) were measured in three to five regions within two to three sequential sections from each tumor biopsy that contained viable tumor cells as described in PATIENTS AND METHODS. Open Columns, mean of pretreatment levels; shaded columns, mean of posttreatment levels. Bars, SD. Note that tumor from patient 9 had the largest (significant) increase in endothelial cell apoptosis. *C,* LSC-mediated quantification of tumor cell apoptosis. Percentages of $CD31^-/TUNEL^+$ cells (mainly tumor cells) were determined in three to five regions within two to three sequential sections from each tumor biopsy that contained viable tumor cells. Open bars, mean of pretreatment levels; shaded bars, mean of posttreatment levels. Bars, SD. Note that treatment-induced changes in tumor cell death were uniformly low across the entire panel, consistent with the lack of clinical activity observed in these trials.

measurement of receptor phosphorylation based on immunofluorescence staining with phosphorylation site–specific antibodies and LSC-mediated quantitative analysis. We then characterized the effects of SU6668 on receptor phosphorylation and growth in orthotopic human L3.5pl pancreatic tumor xenografts. Although there seemed to be a modest (but not significant) dose-dependent inhibition of tumor MVDs at 25 and 50 mg/kg, significant reductions in MVD (26%) and tumor growth (40%) were only observed in tumors treated with SU6668 maximum tolerated dose (100 mg/kg). The effects were associated with marked (5-fold) increases in endothelial cell apoptosis and impressive (1.7-fold) increases in tumor cell death, consistent with previous work implicating endothelial cell apoptosis in the antitumor activity of SU6668 in other models (14, 15). We then characterized the time-dependent inhibitory effects of SU6668 on VEGFR-2 and PDGFR-β phosphorylation. As expected, levels of active VEGFR-2 and PDGFR were reduced by 50% in endothelial cells, and PDGFR phosphorylation was reduced by over 90% in tumor cells 6 hours after drug dosing. Strikingly, however, this inhibition of receptor phosphorylation was not sustained, and, in fact, levels of active VEGFR-2 and PDGFR were found to be significantly higher than controls in tumors

24 hours after therapy. Thus, SU6668-mediated inhibition of receptor activation probably resulted in positive feedback mechanisms that drove higher levels of receptor phosphorylation once the inhibitor was cleared. Positive feedback mechanisms might also underlie the enhanced total VEGFR-2 expression observed in xenografts treated with the blocking anti-VEGFR-2 antibody DC101 (25) and the increases in serum VEGF levels that were observed in patients treated with SU5416 (17). They could also have important implications for tumor growth and angiogenesis following cessation of therapy with receptor tyrosine kinase inhibitors.

We next measured the effects of SU5416 and SU6668 in biopsies obtained from patients enrolled in clinical trials. In one set of biopsies (patient 2) we observed parallel decreases in VEGFR-2 and PDGFR phosphorylation that were associated with decreased MVD, but these effects did not translate into increased endothelial cell death. Without having multiple posttreatment biopsies available, we cannot exclude the possibility that the levels of cell death actually did increase in tumor 2 at a time point we did not analyze. Alternatively, it is possible that the transient nature of SU6668-mediated receptor inhibition was insufficient to trigger significant cell death in tumor 2. Given that this tumor did not respond to SU6668 therapy, we favor the latter hypothesis.

In another biopsy set (patient 9), SU5416 therapy was associated with decreased MVD, increased vessel size, and increased endothelial cell death. However, quantitative analyses of VEGFR-2 phosphorylation did not show target inhibition in this or any of the other biopsy sets obtained from the patients treated with SU5416. Because SU5416 IC_{50} value for VEGFR-2 (0.16 μmol/L) is lower than that of SU6668 (2.1 μmol/L), we expected that at maximum tolerated doses of each drug we would observe stronger inhibition of VEGFR-2 phosphorylation in the tumors exposed to SU5416. The most likely explanation for the discrepancy between the VEGFR-2 phosphorylation and MVD/endothelial cell death results in tumor 9 is that the follow-up biopsy was obtained too long (>3 days) after SU5416 dosing to allow us to detect inhibition of receptor activation. The lack of a clinical response in this tumor can be explained by the fact that the vascular changes were not associated with increased tumor cell death, most likely because disease progression and/or prior therapy had already selected for the expansion of cells with a death-resistant phenotype. We observed a very similar uncoupling of endothelial and tumor cell death in posttreatment biopsies obtained within the context of a phase I dose-escalation trial with recombinant human endostatin (24).

The effects of SU6668 on VEGFR-2 and PDGFR phosphorylation were quite heterogeneous in the group of patients that all received the same dose of drug (200 mg/m^2). Our results are reminiscent of recent studies on the effects of EGFR inhibitors on EGFR activation in skin versus tumor biopsies. In studies of OSI-774 or ZD1839/Iressa, multiple parameters of EGFR activation were suppressed in all skin biopsies (34, 35), whereas evidence for receptor inhibition was obtained in a minority of tumor samples collected from patients treated with ZD1839 in a separate trial (36). Together, the data strongly suggest that intertumor heterogeneity in drug-target interactions and subsequent biological responses is one factor that limits clinical activity in trials with these agents.

Although the importance of obtaining pharmacodynamic evidence of drug targeting in studies with receptor tyrosine kinase antagonists would seem self-evident from a scientific/theoretical standpoint (37, 38), the practical value of biopsy-based pharmacodynamic studies remains a major point of contention. Interest in measuring pharmacodynamic end points invasively is tempered by concern for patient safety, and the validity and predictive value of the assays used in such studies is still unclear. Ongoing studies are performing pharmacodynamic analyses of drug-target interactions in a phase II trial of Gleevec in patients with gastrointestinal stromal tumors. Because Gleevec has major clinical and pharmacodynamic activity in this disease (39–41), our approach should allow us to directly assess the relationships between changes in receptor phosphorylation, apoptosis, and clinical response.

REFERENCES

1. Folkman J. Tumor angiogenesis: therapeutic implications. N Engl J Med 1971;285:1182–6.

2. Folkman J. Tumor angiogenesis. Adv Cancer Res 1985;43:175–203.

3. Folkman J. Angiogenesis in cancer, vascular, rheumatoid and other disease. Nat Med 1995;1:27–31.

4. Hanahan D, Folkman J. Patterns and emerging mechanisms of the angiogenic switch during tumorigenesis. Cell 1996;86:353–64.

5. Fidler IJ, Singh RK, Yoneda J, et al. Critical determinants of neoplastic angiogenesis. Cancer J 2000;6 Suppl 3:S225–36.

6. Dvorak HF. Vascular permeability factor/vascular endothelial growth factor: a critical cytokine in tumor angiogenesis and a potential target for diagnosis and therapy. J Clin Oncol 2002;20:4368–80.

7. Glade-Bender J, Kandel JJ, Yamashiro DJ. VEGF blocking therapy in the treatment of cancer. Expert Opin Biol Ther 2003;3:263–76.

8. Stadler W, Wilding G. Angiogenesis inhibitors in genitourinary cancers. Crit Rev Oncol Hematol 2003;46:S41–7.

9. Fong TA, Shawver LK, Sun L, et al. SU5416 is a potent and selective inhibitor of the vascular endothelial growth factor receptor (Flk-1/KDR) that inhibits tyrosine kinase catalysis, tumor vascularization, and growth of multiple tumor types. Cancer Res 1999;59:99–106.

10. Laird AD, Vajkoczy P, Shawver LK, et al. SU6668 is a potent antiangiogenic and antitumor agent that induces regression of established tumors. Cancer Res 2000;60:4152–60.

11. Sun L, Tran N, Tang F, et al. Synthesis and biological evaluations of 3-substituted indolin-2-ones: a novel class of tyrosine kinase inhibitors that exhibit selectivity toward particular receptor tyrosine kinases. J Med Chem 1998;41:2588–603.

12. Angelov L, Salhia B, Roncari L, McMahon G, Guha A. Inhibition of angiogenesis by blocking activation of the vascular endothelial growth factor receptor 2 leads to decreased growth of neurogenic sarcomas. Cancer Res 1999;59:5536–41.

13. Mendel DB, Schreck RE, West DC, et al. The angiogenesis inhibitor SU5416 has long-lasting effects on vascular endothelial growth factor receptor phosphorylation and function. Clin Cancer Res 2000;6:4848–58.

14. Shaheen RM, Davis DW, Liu W, et al. Antiangiogenic therapy targeting the tyrosine kinase receptor for vascular endothelial growth factor receptor inhibits the growth of colon cancer liver metastasis and induces tumor and endothelial cell apoptosis. Cancer Res 1999;59:5412–6.

15. Laird AD, Christensen JG, Li G, et al. SU6668 inhibits Flk-1/KDR and PDGFRβ *in vivo*, resulting in rapid apoptosis of tumor vasculature and tumor regression in mice. FASEB J 2002;16:681–90.

16. Stadler WM, Cao D, Vogelzang NJ, et al. A randomized phase II trial of the antiangiogenic agent SU5416 in hormone-refractory prostate cancer. Clin Cancer Res 2004;10:3365–70.

17. Peterson AC, Swiger S, Stadler WM, Medved M, Karczmar G, Gajewski TF. Phase II study of the Flk-1 tyrosine kinase inhibitor SU5416 in advanced melanoma. Clin Cancer Res 2004;10:4048–54.

18. Heymach JV, Desai J, Manola J, et al. Phase II study of the antiangiogenic agent SU5416 in patients with advanced soft tissue sarcomas. Clin Cancer Res 2004;10:5732–40.

19. Xiong HQ, Herbst R, Faria SC, et al. A phase I surrogate endpoint study of SU6668 in patients with solid tumors. Invest New Drugs 2004; 22:459–66.

20. Baker CH, Solorzano CC, Fidler IJ. Blockade of vascular endothelial growth factor receptor and epidermal growth factor receptor signaling for therapy of metastatic human pancreatic cancer. Cancer Res 2002;62: 1996–2003.

21. Solorzano CC, Baker CH, Bruns CJ, et al. Inhibition of growth and metastasis of human pancreatic cancer growing in nude mice by PTK 787/ZK222584, an inhibitor of the vascular endothelial growth factor receptor tyrosine kinases. Cancer Biother Radiopharm 2001;16: 359–70.

22. Hwang RF, Yokoi K, Bucana CD, et al. Inhibition of platelet-derived growth factor receptor phosphorylation by STI571 (Gleevec) reduces growth and metastasis of human pancreatic carcinoma in an orthotopic nude mouse model. Clin Cancer Res 2003;9:6534–44.

23. Davis DW, Buchholz TA, Hess KR, Sahin AA, Valero V, McConkey DJ. Automated quantification of apoptosis after neoadjuvant chemotherapy for breast cancer: early assessment predicts clinical response. Clin Cancer Res 2003;9:955–60.

24. Davis DW, Shen Y, Mullani NA, et al. Quantitative analysis of biomarkers defines an optimal biological dose for recombinant human endostatin in primary human tumors. Clin Cancer Res 2004;10:33–42.

25. Davis DW, Inoue K, Dinney CP, Hicklin DJ, Abbruzzese JL, McConkey DJ. Regional effects of an antivascular endothelial growth factor receptor monoclonal antibody on receptor phosphorylation and apoptosis in human 253J B-V bladder cancer xenografts. Cancer Res 2004;64:4601–10.

26. Bruns CJ, Harbison MT, Kuniyasu H, Eue I, Fidler IJ. *In vivo* selection and characterization of metastatic variants from human pancreatic adenocarcinoma by using orthotopic implantation in nude mice. Neoplasia 1999;1:50–62.

27. Nawrocki ST, Bruns CJ, Harbison MT, et al. Effects of the proteasome inhibitor PS-341 on apoptosis and angiogenesis in orthotopic human pancreatic tumor xenografts. Mol Cancer Ther 2002;1:1243–53.

28. Bruns CJ, Solorzano CC, Harbison MT, et al. Blockade of the epidermal growth factor receptor signaling by a novel tyrosine kinase inhibitor leads to apoptosis of endothelial cells and therapy of human pancreatic carcinoma. Cancer Res 2000;60:2926–35.

29. Drevs J, Muller-Driver R, Wittig C, et al. PTK787/ZK 222584, a specific vascular endothelial growth factor-receptor tyrosine kinase inhibitor, affects the anatomy of the tumor vascular bed and the functional vascular properties as detected by dynamic enhanced magnetic resonance imaging. Cancer Res 2002;62:4015–22.

30. Ferrara N. VEGF and the quest for tumour angiogenesis factors. Nat Rev Cancer 2002;2:795–803.

31. Ferrara N, Gerber HP, LeCouter J. The biology of VEGF and its receptors. Nat Med 2003;9:669–76.

32. Stopeck A, Sheldon M, Vahedian M, Cropp G, Gosalia R, Hannah A. Results of a phase I dose-escalating study of the antiangiogenic agent, SU5416, in patients with advanced malignancies. Clin Cancer Res 2002;8:2798–805.

33. Mesters RM, Padro T, Bieker R, et al. Stable remission after administration of the receptor tyrosine kinase inhibitor SU5416 in a patient with refractory acute myeloid leukemia. Blood 2001;98: 241–3.

34. Albanell J, Rojo F, Averbuch S, et al. Pharmacodynamic studies of the epidermal growth factor receptor inhibitor ZD1839 in skin from cancer patients: histopathologic and molecular consequences of receptor inhibition. J Clin Oncol 2002;20:110–24.

35. Malik SN, Siu LL, Rowinsky EK, et al. Pharmacodynamic evaluation of the epidermal growth factor receptor inhibitor OSI-774 in human epidermis of cancer patients. Clin Cancer Res 2003;9: 2478–86.

36. Daneshmand M, Parolin DA, Hirte HW, et al. A pharmacodynamic study of the epidermal growth factor receptor tyrosine kinase inhibitor ZD1839 in metastatic colorectal cancer patients. Clin Cancer Res 2003;9: 2457–64.

37. Herbst RS, Mullani NA, Davis DW, et al. Development of biologic markers of response and assessment of antiangiogenic activity in a clinical trial of human recombinant endostatin. J Clin Oncol 2002;20: 3804–14.

38. Davis DW, McConkey DJ, Abbruzzese JL, Herbst RS. Surrogate markers in antiangiogenesis clinical trials. Br J Cancer 2003;89:8–14.

39. Demetri GD. Targeting c-kit mutations in solid tumors: scientific rationale and novel therapeutic options. Semin Oncol 2001;28:19–26.

40. Heinrich MC, Corless CL, Demetri GD, et al. Kinase mutations and imatinib response in patients with metastatic gastrointestinal stromal tumor. J Clin Oncol 2003;21:4342–9.

41. Frolov A, Chahwan S, Ochs M, et al. Response markers and the molecular mechanisms of action of Gleevec in gastrointestinal stromal tumors. Mol Cancer Ther 2003;2:699–709.

Clinical Cancer Research

Pharmacodynamic Analysis of Target Inhibition and Endothelial Cell Death in Tumors Treated with the Vascular Endothelial Growth Factor Receptor Antagonists SU5416 or SU6668

Darren W. Davis, Ryan Takamori, Chandrajit P. Raut, et al.

Clin Cancer Res 2005;11:678-689.